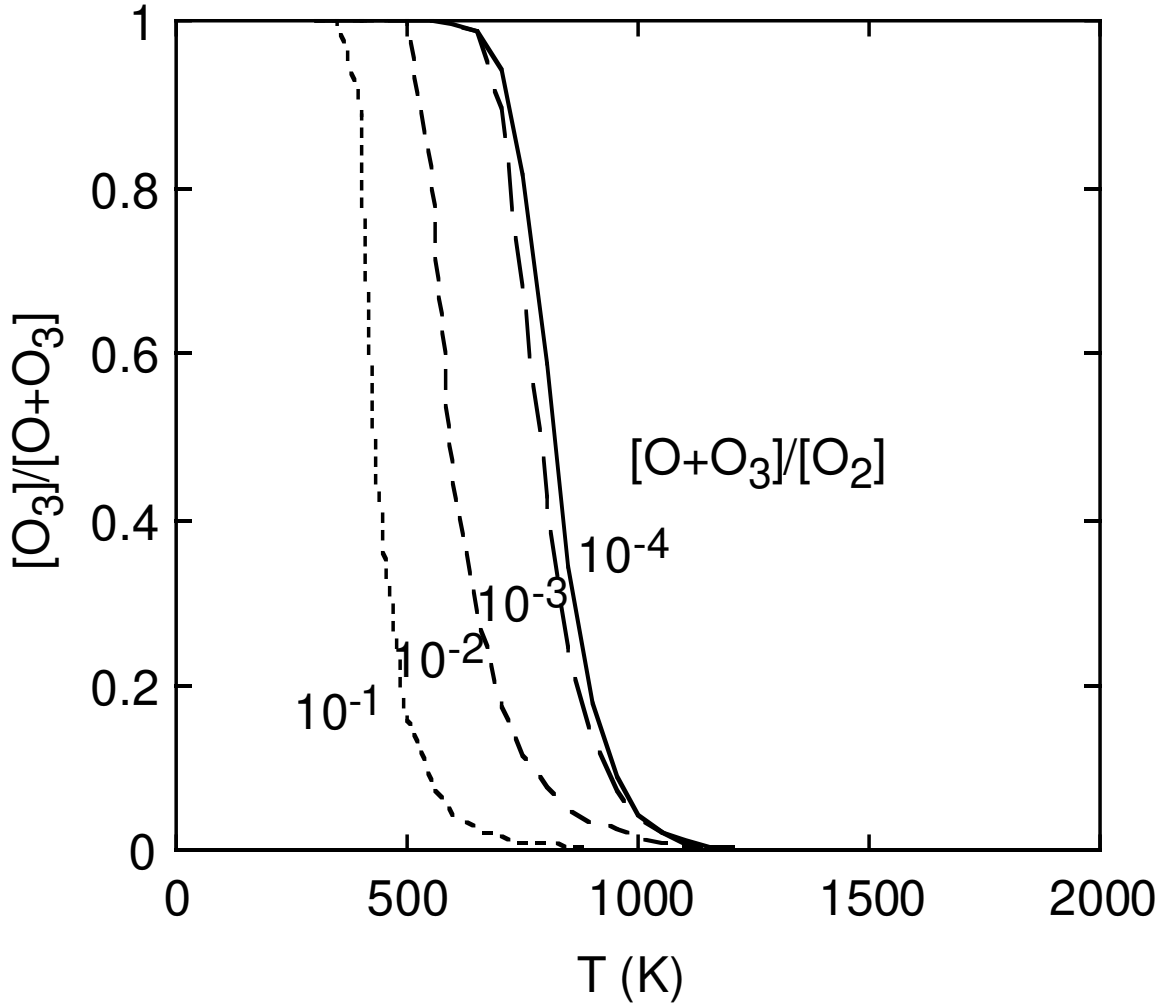

PPPL/3281/Fig. 1: $[O_3]/[O + O_3]$ as a function of temperature for a range of values of $[O + O_3]/[O_2]$.

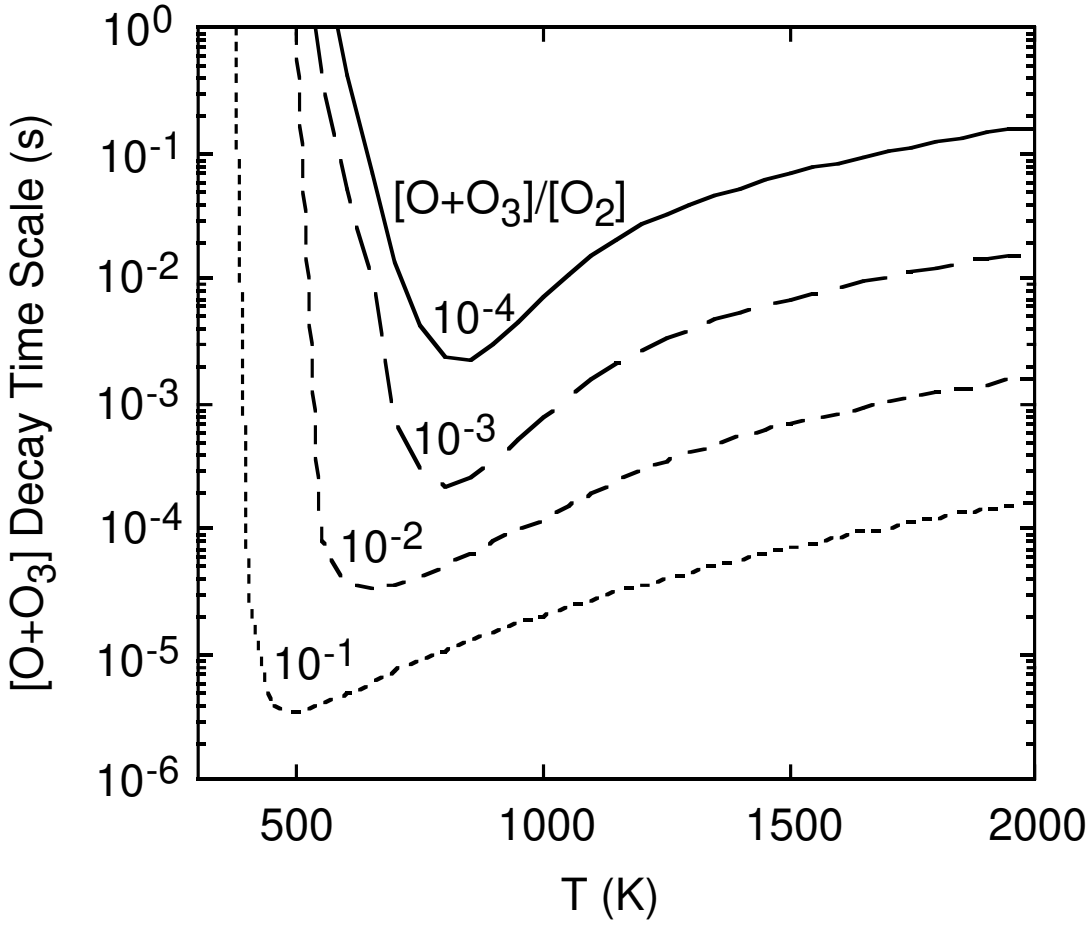

PPPL-3281/Fig. 2: Dependence of [O + O_3] destruction time scale, τ_{des}, on temperature for a range of values of [O + O_3]/[O_2].

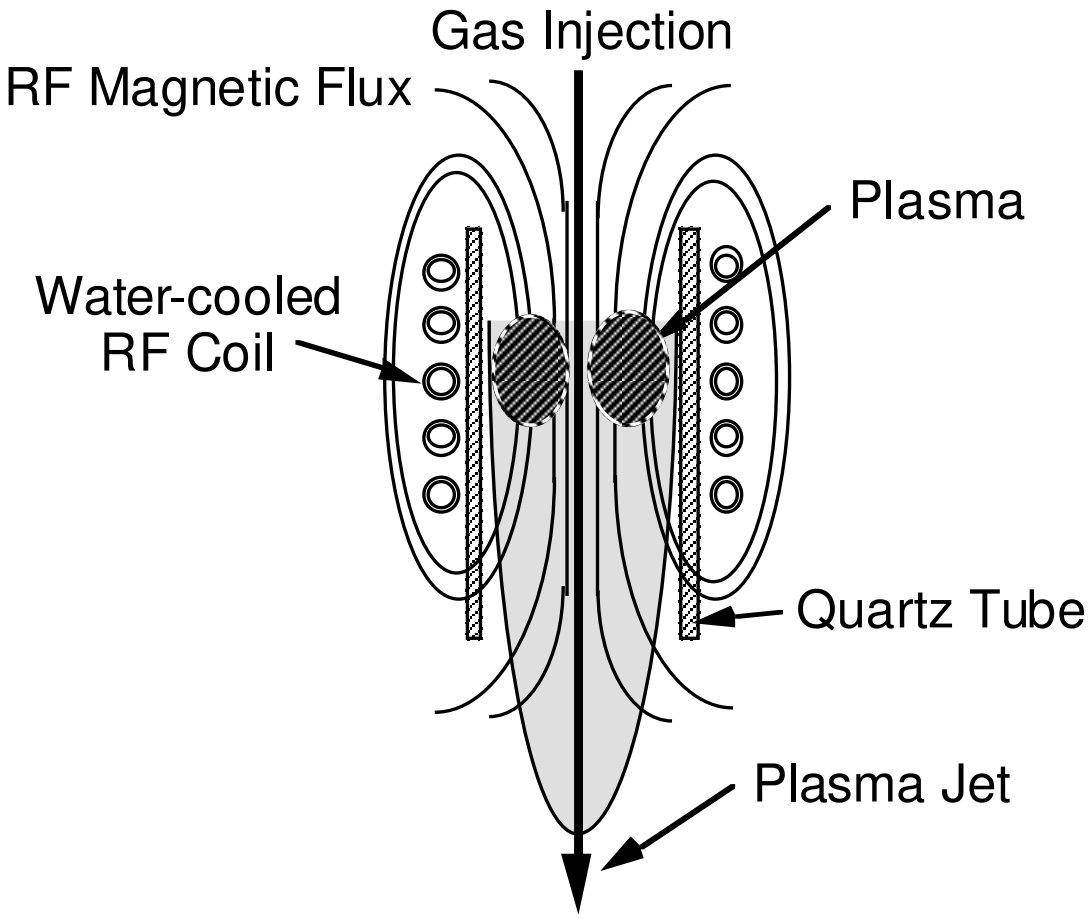

PPPL-3281/Fig. 3: Schematic of an RF induction-coupled plasma (ICP) torch.

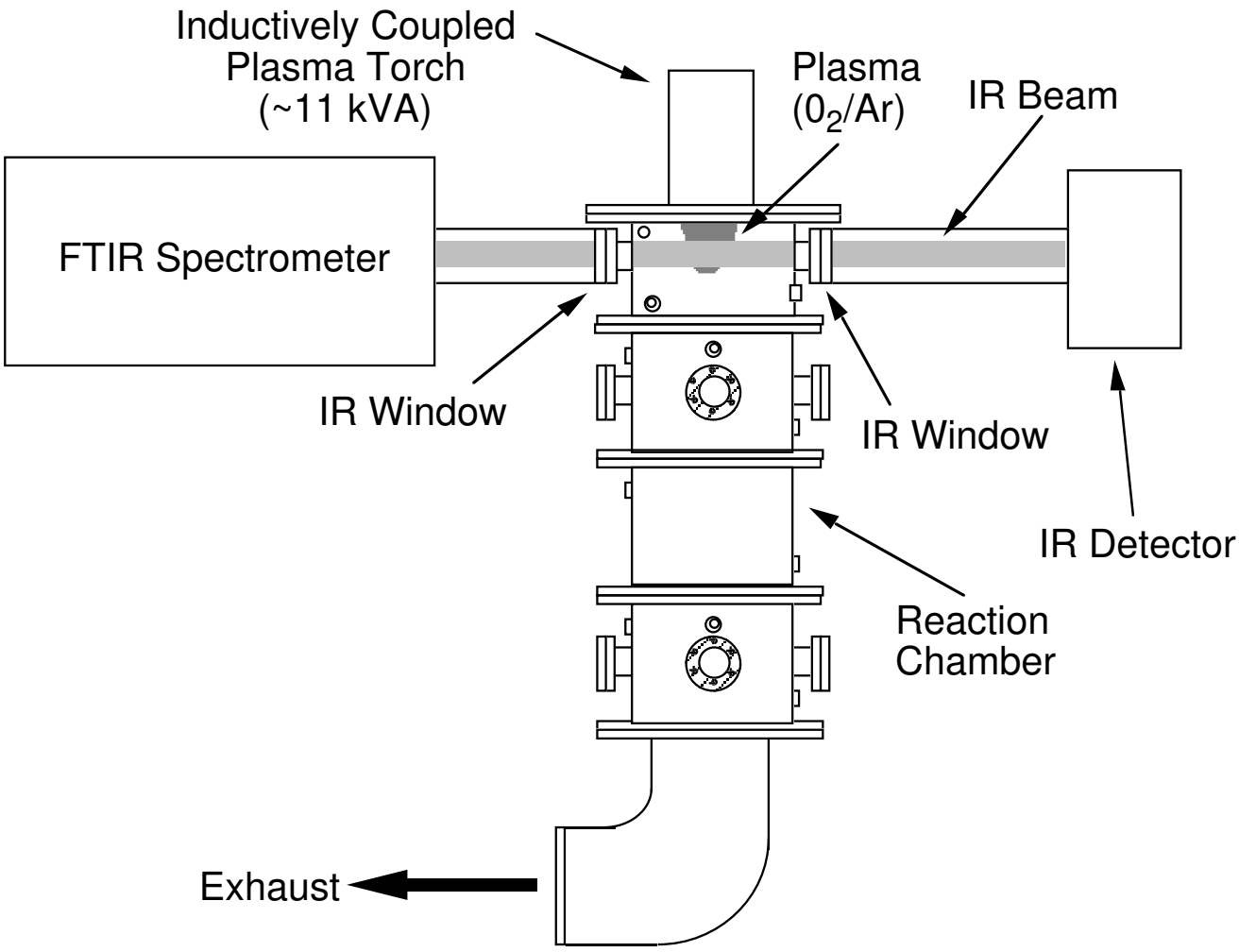

PPPL-3281/Fig. 4: Schematic of ozone production experiment showing ICP torch, reactor chamber, and FTIR spectrometer.

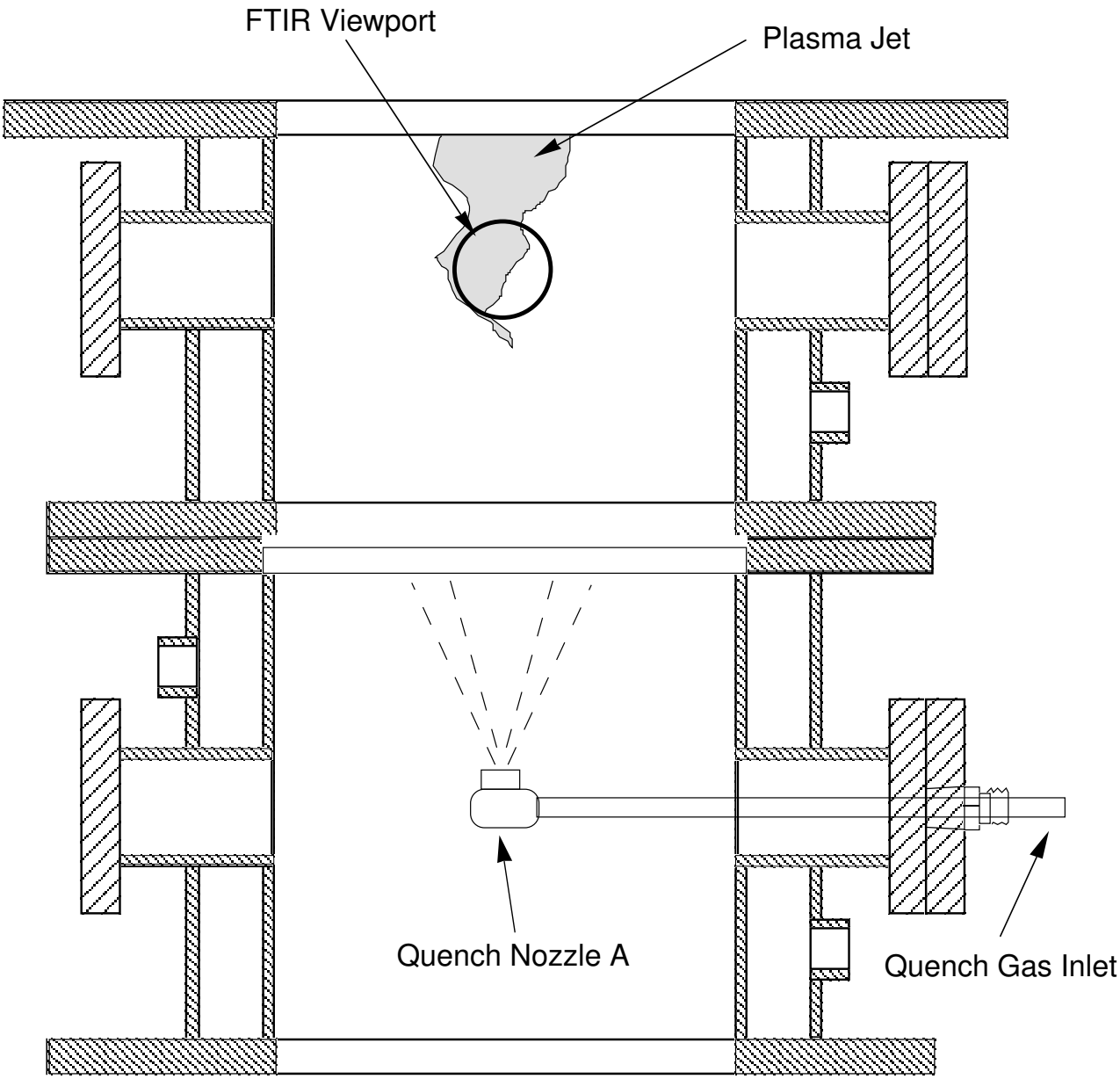

PPPL-3281/Fig. 5a: Quench nozzle A.

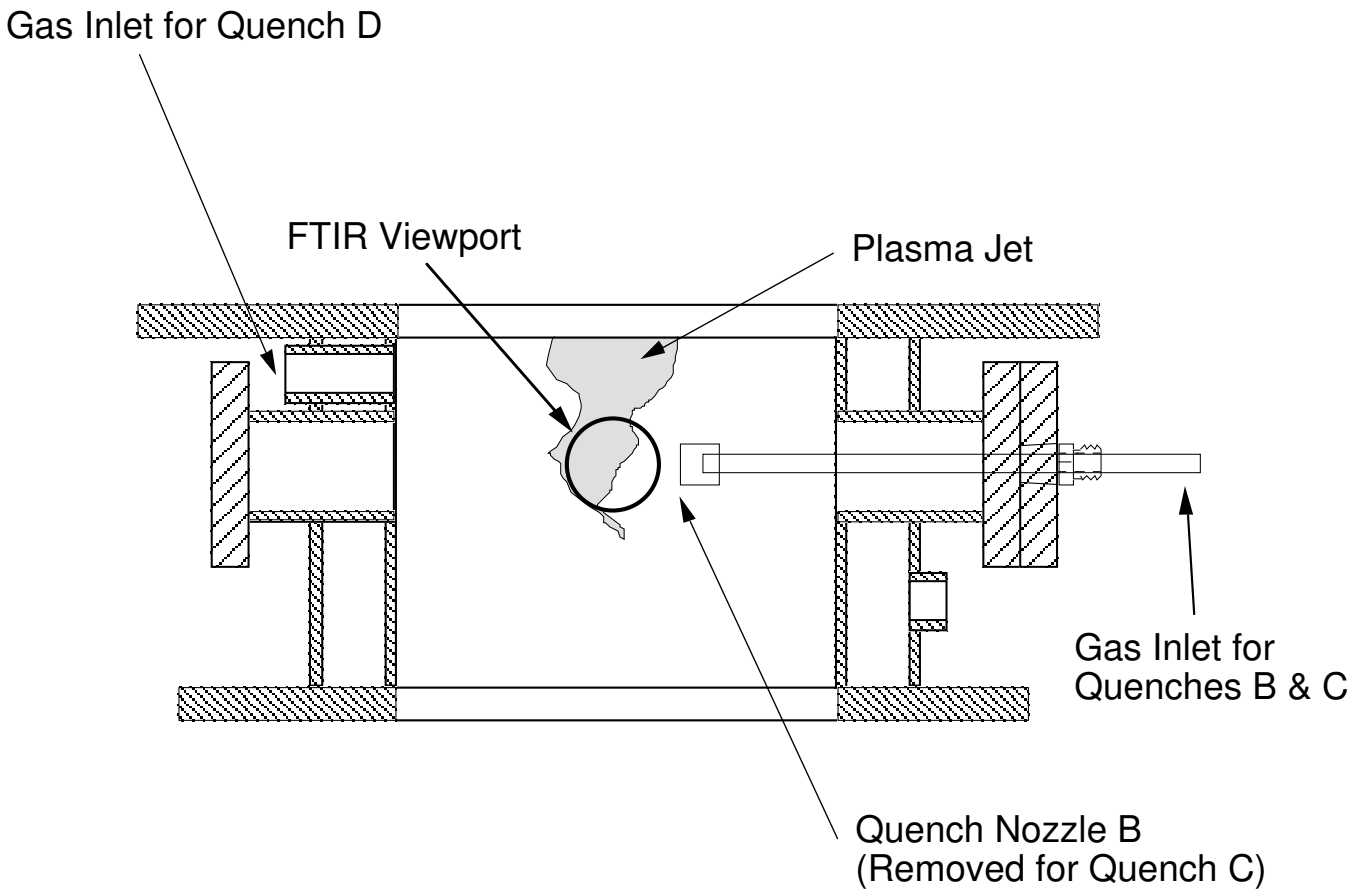

PPPL-3281/Fig. 5b: Quench nozzle B (used cap with 2 mm diameter orifice) and quench nozzle C (without cap; 4.5 mm ID tube acting as orifice). Quench D utilized the 16 mm diameter port.

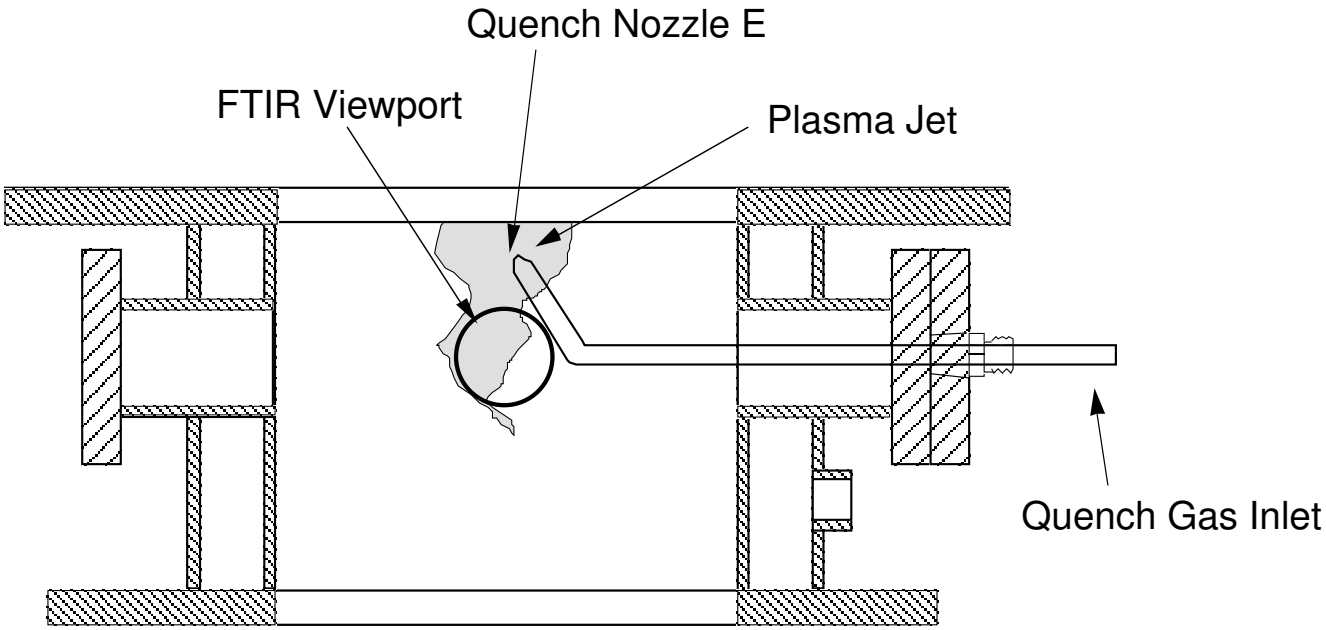

PPPL-3281/Fig. 5c: Quench nozzle E.

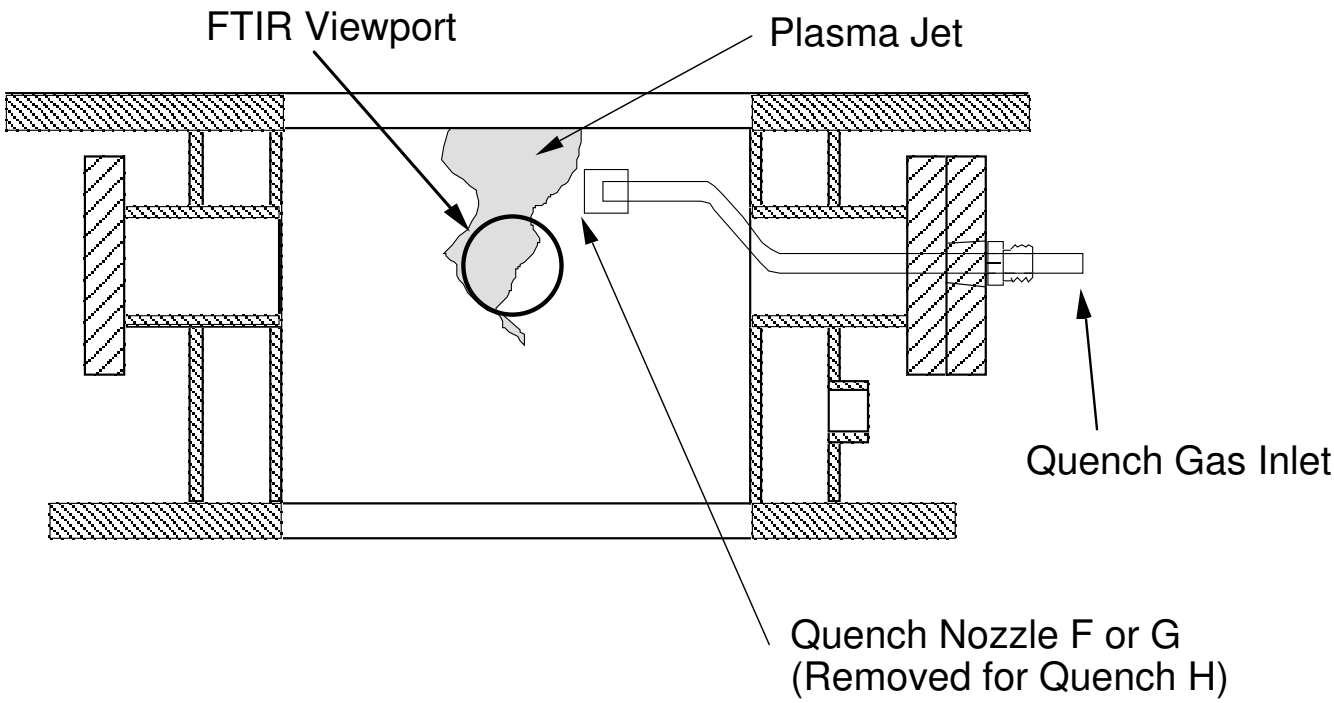

PPPL-3281/Fig. 5d: Quench nozzle F (used cap with 1.1 mm diameter orifice); quench nozzle G (used cap with 2.2 mm diameter orifice); quench H (without cap; 3.2 mm inner diameter tube acting as orifice).

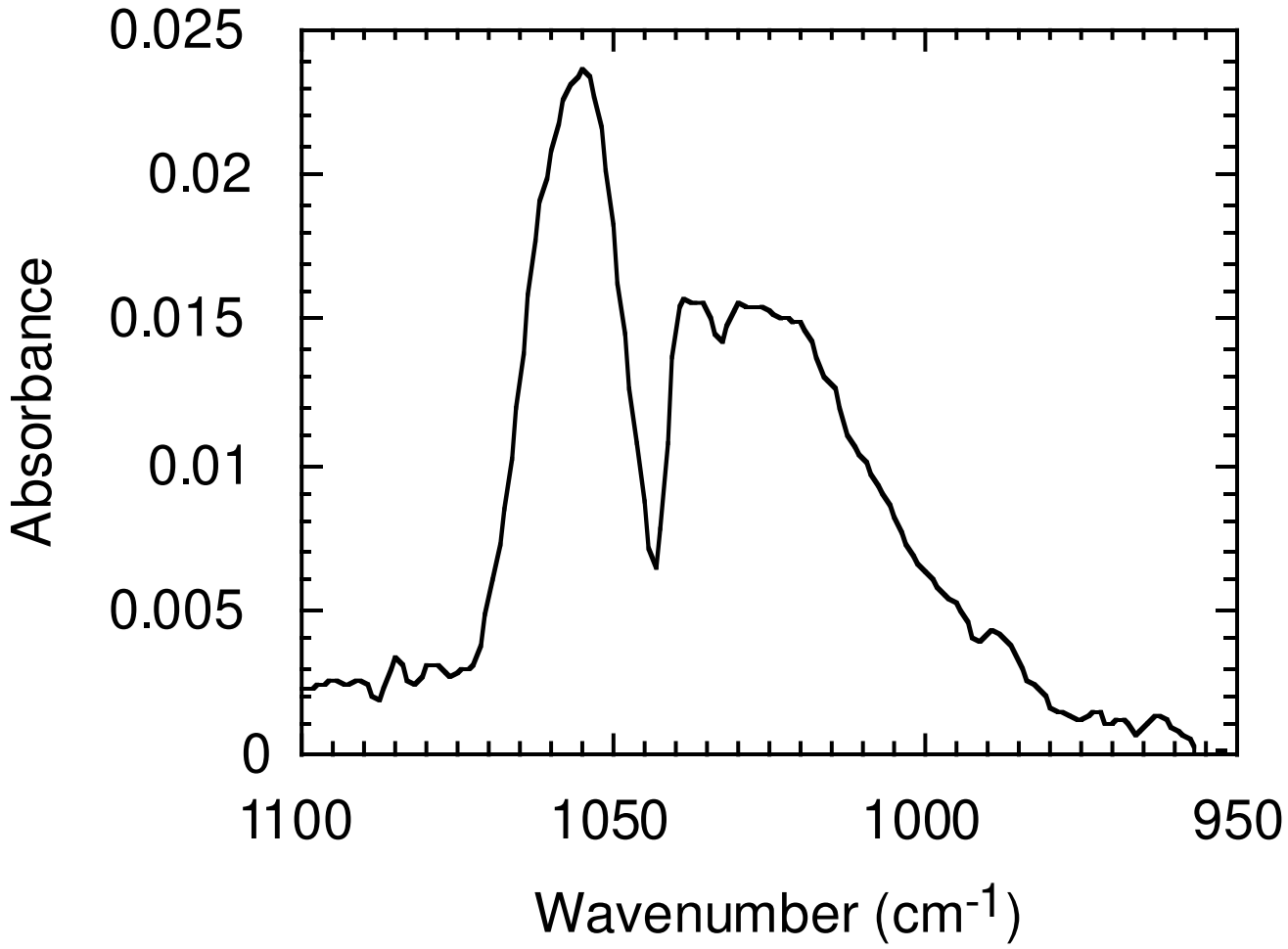

PPPL-3281/Fig. 6: FTIR spectrum of ozone antisymmetric stretching band at 1042 cm^{-1}. An ozone concentration of 220 ppm was deduced fromthis measurement.

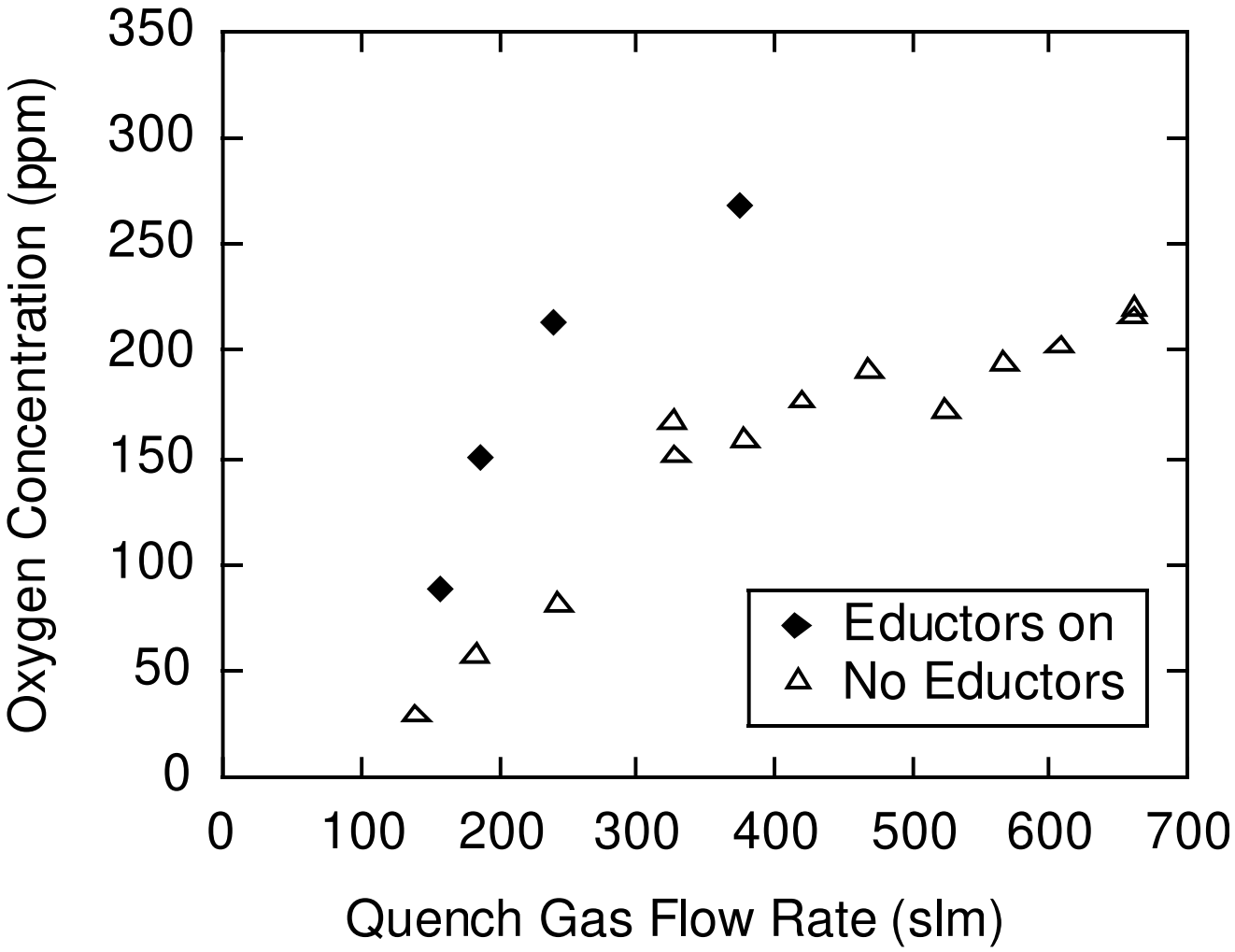

PPPL-3281/Fig. 7: Dependence of ozone concentration on oxygen quench gas flow ratefor quench nozzle A operated with and without active pumping of the reactor.

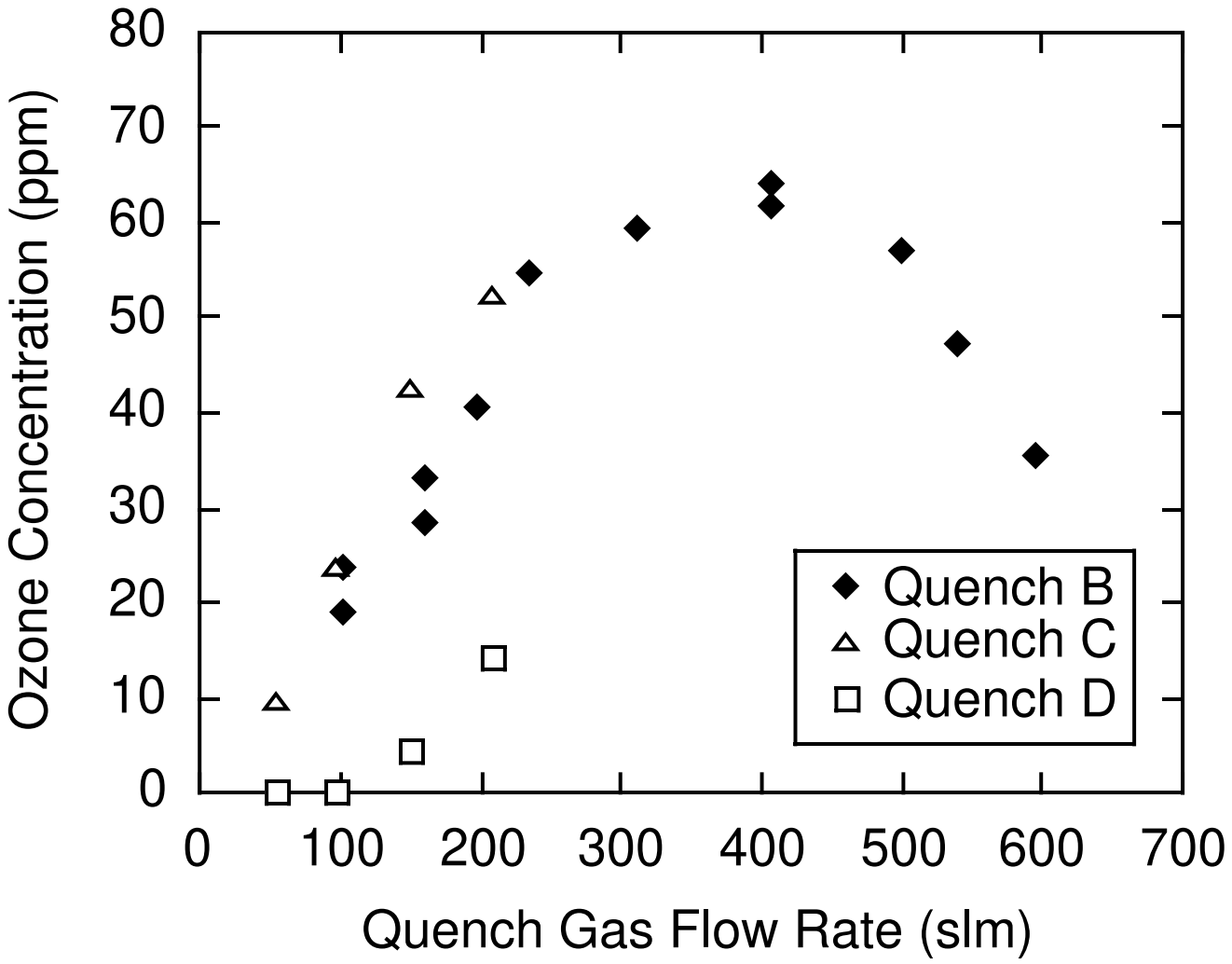

PPPL-3281/Fig. 8: Dependence of ozone concentration on oxygen quench gas flow rate for quench nozzles B, C, and D.

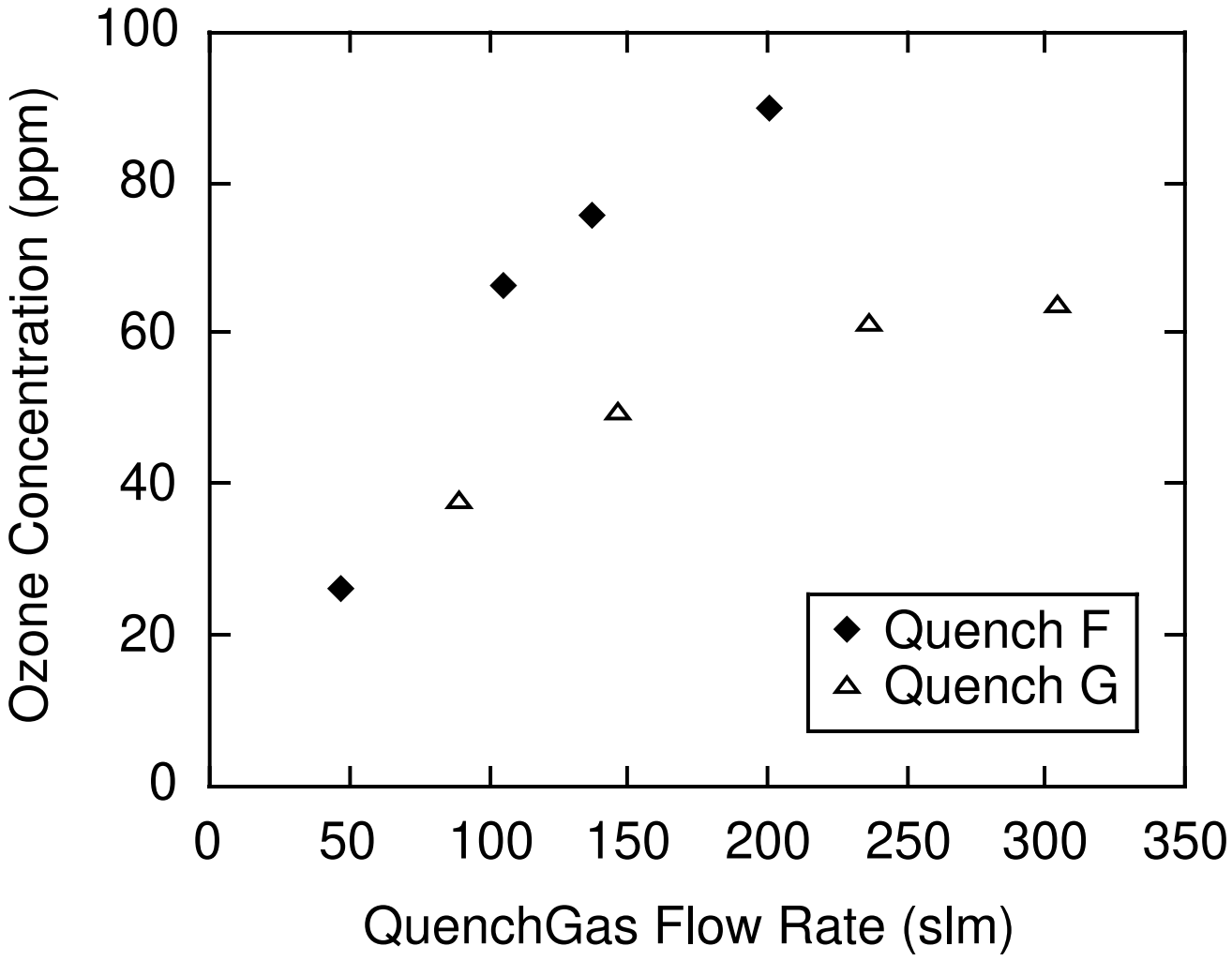

PPPL-3281/Fig. 9: Dependence of ozone concentration on oxygen quench gas flow rate for quench nozzles F and G.

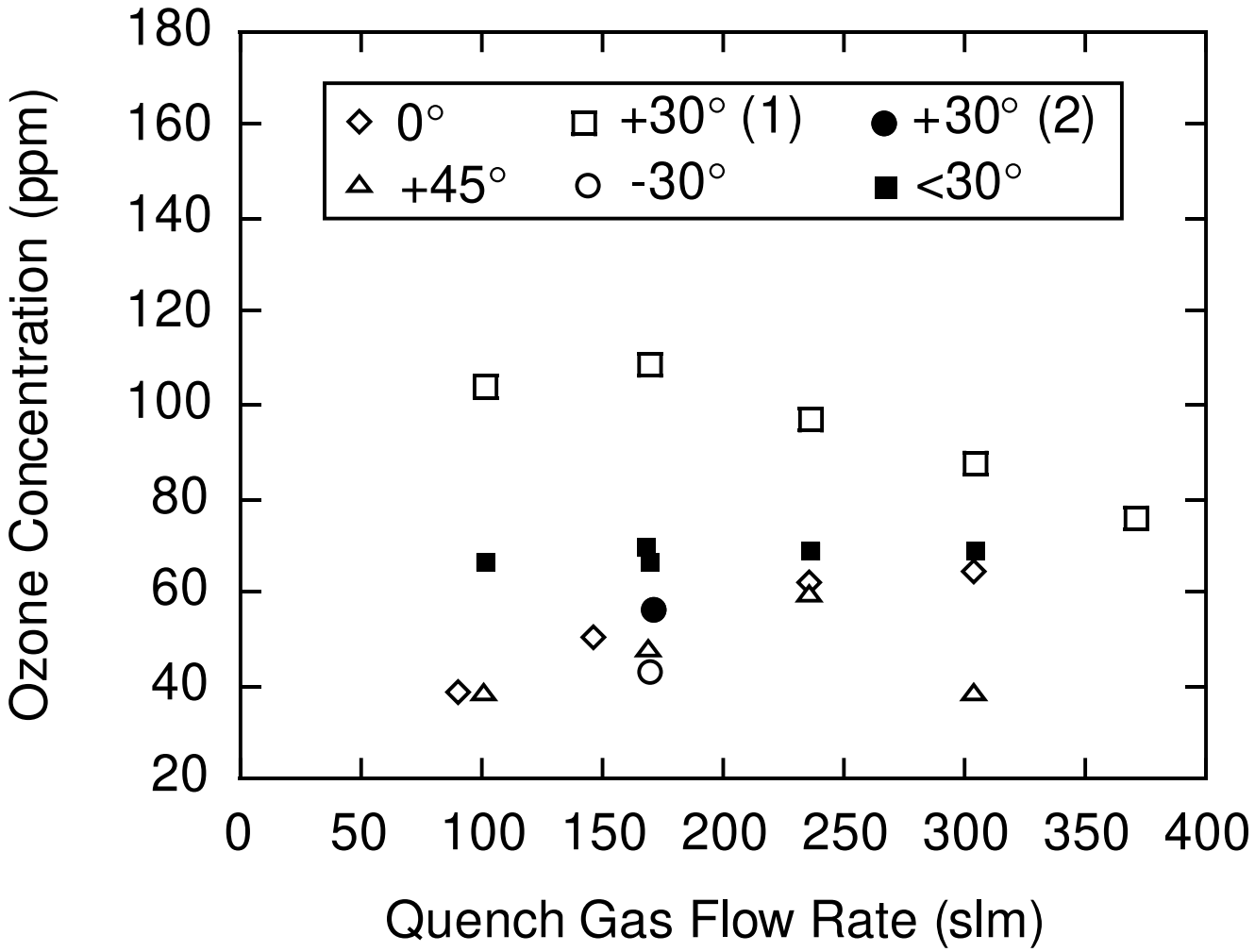

PPPL-3281/Fig. 10: Effect of varying angle of quench nozzle G on ozone concentration.

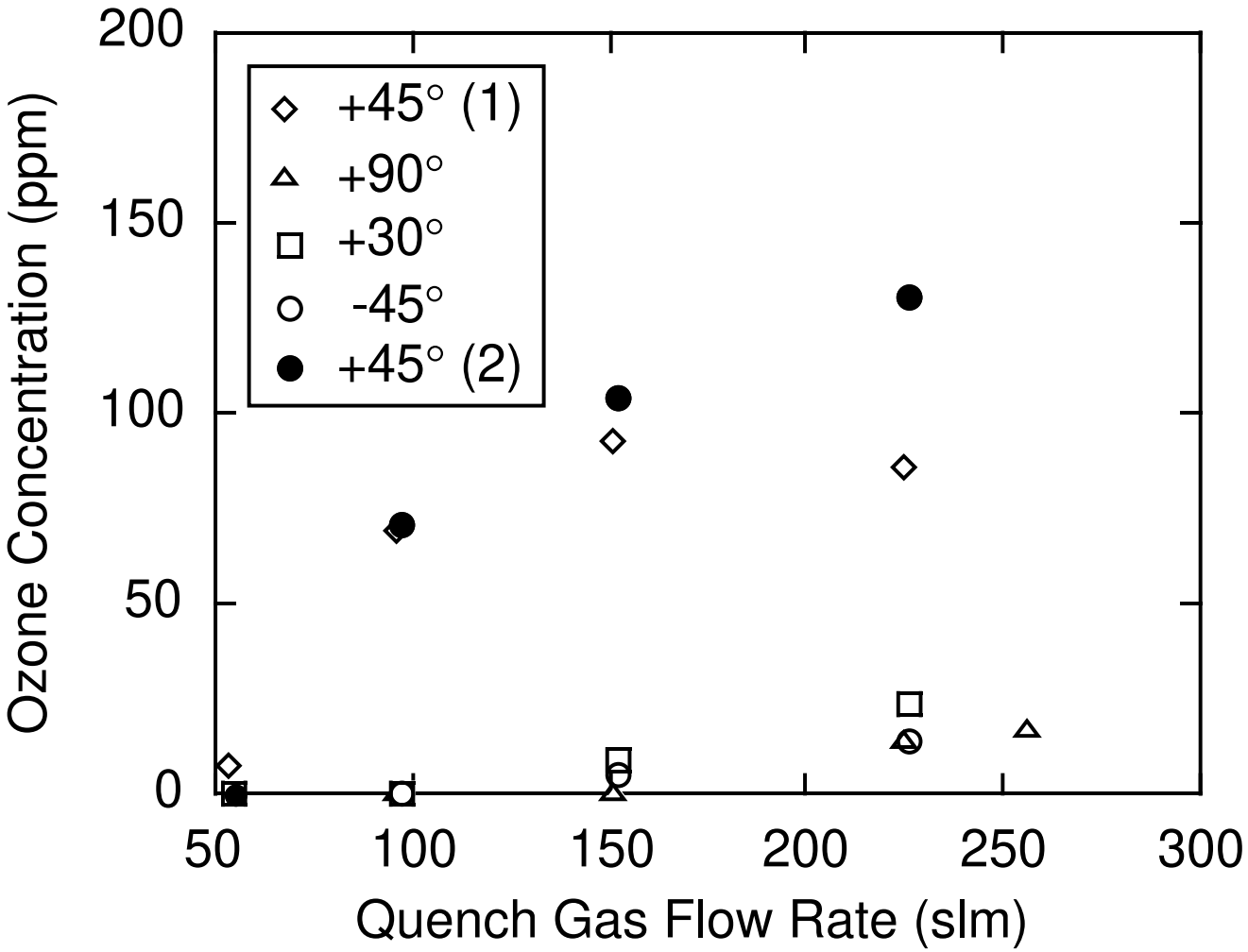

PPPL-3281/Fig. 11: Effect of varying angle of quench nozzle E on ozone concentration.

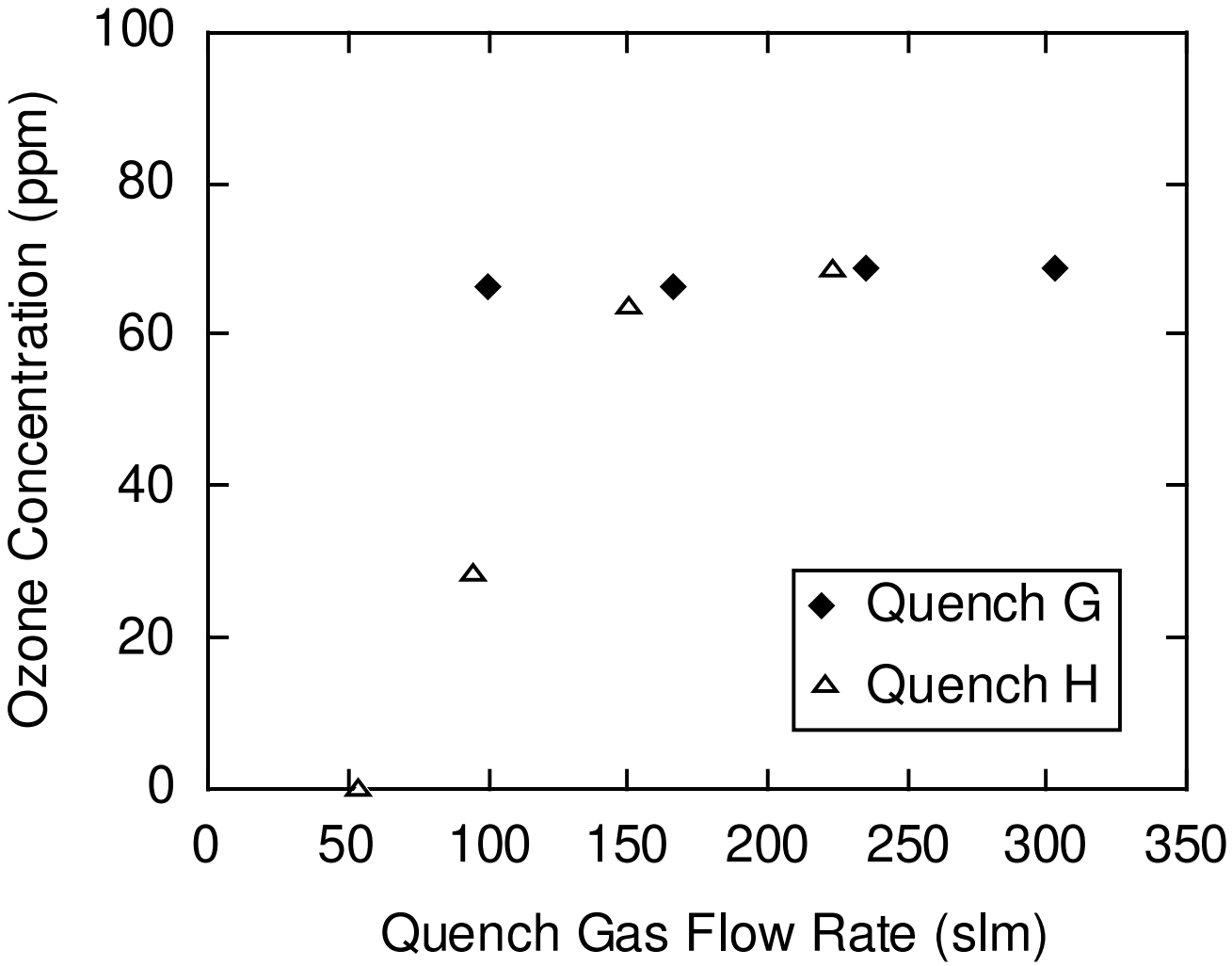

PPPL-3281/Fig. 12: Comparison of ozone concentrations produced by quench nozzles G and H rotated to an angle of +30°.

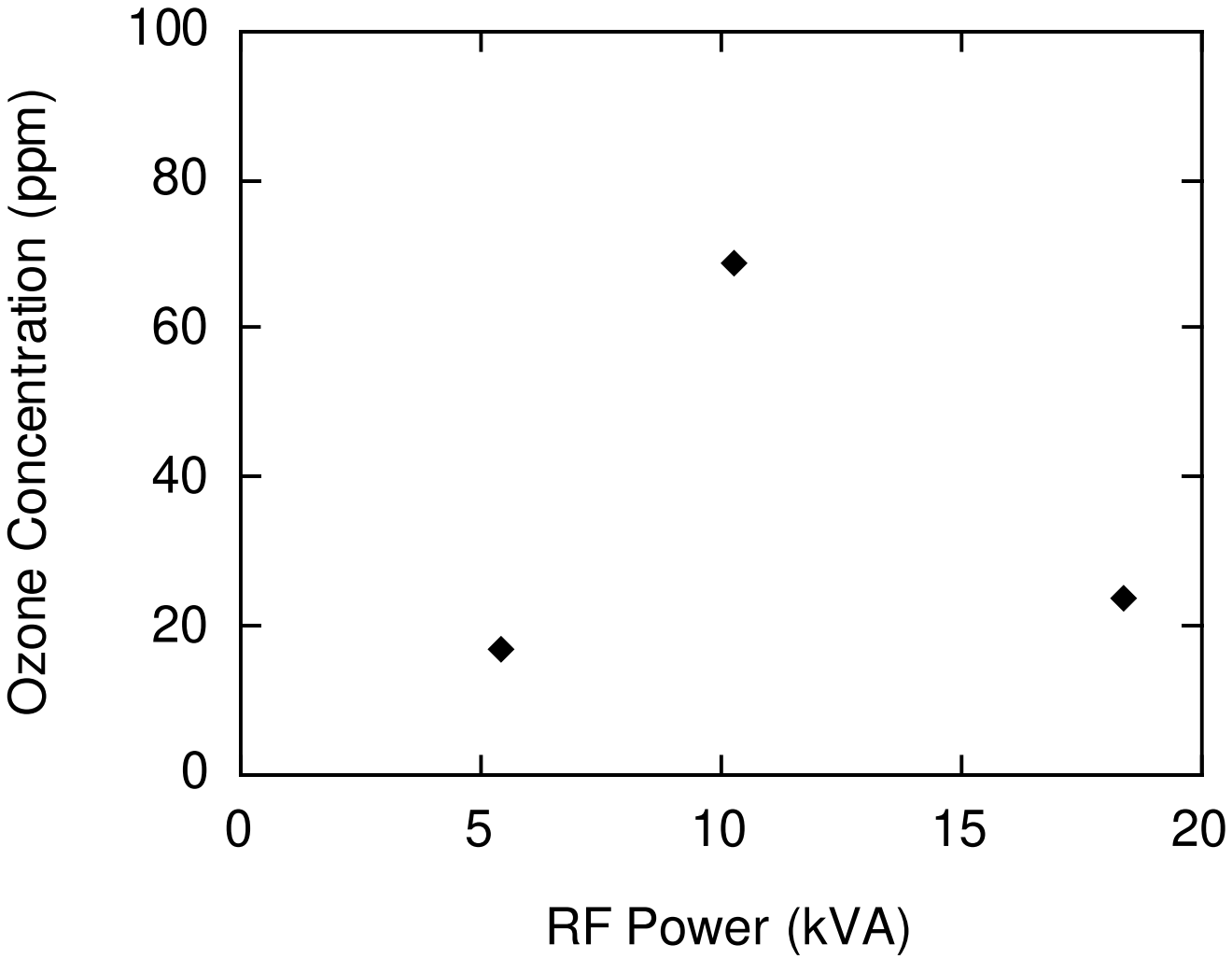

PPPL-3281/Fig. 13: Dependence of ozone concentration on torch power for quench nozzle G rotated to an angle of +30°.

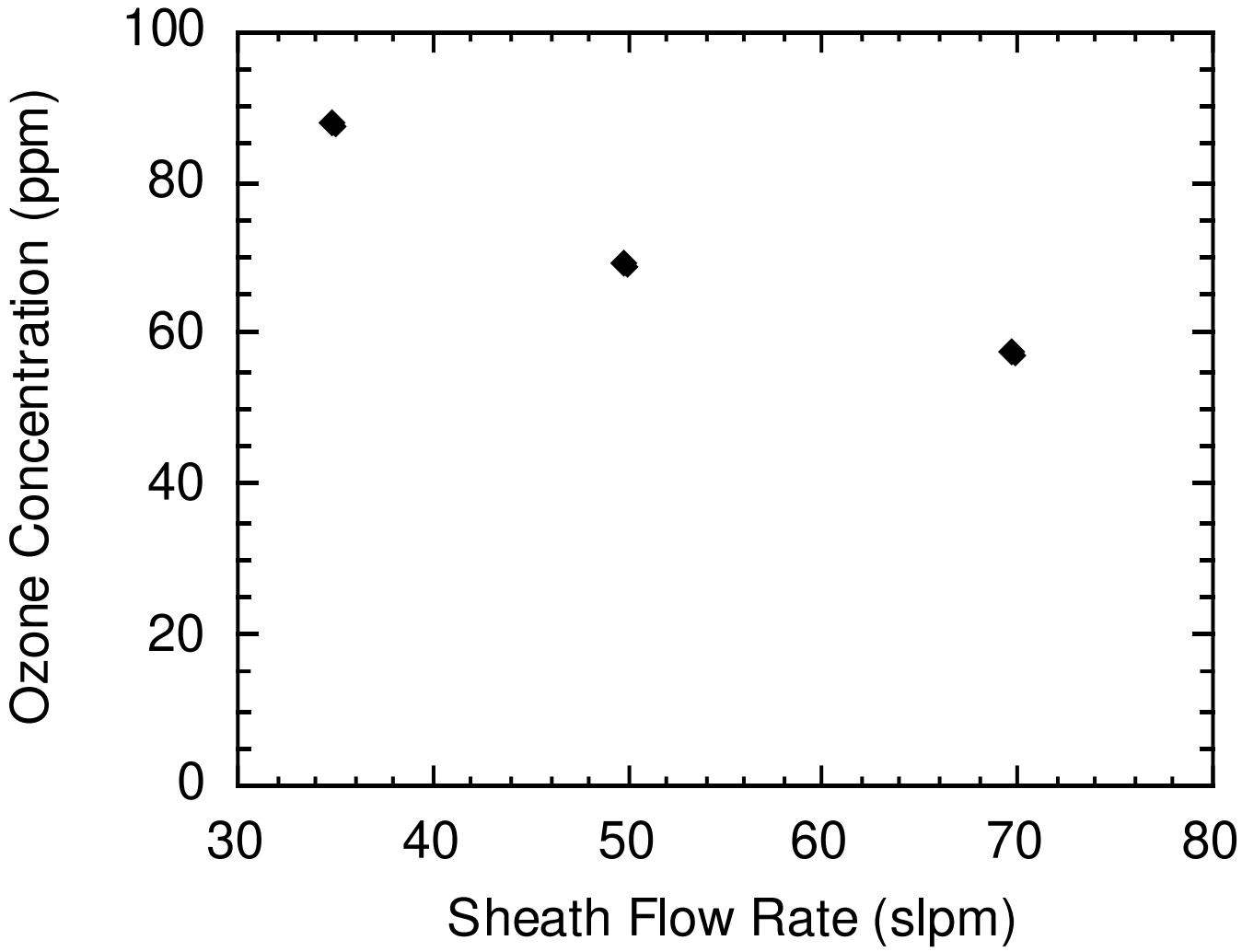

PPPL-3281/Fig. 14: Dependence of ozone concentration on torch sheath gas flow rate for quench nozzle G rotated to an angle of +30°.

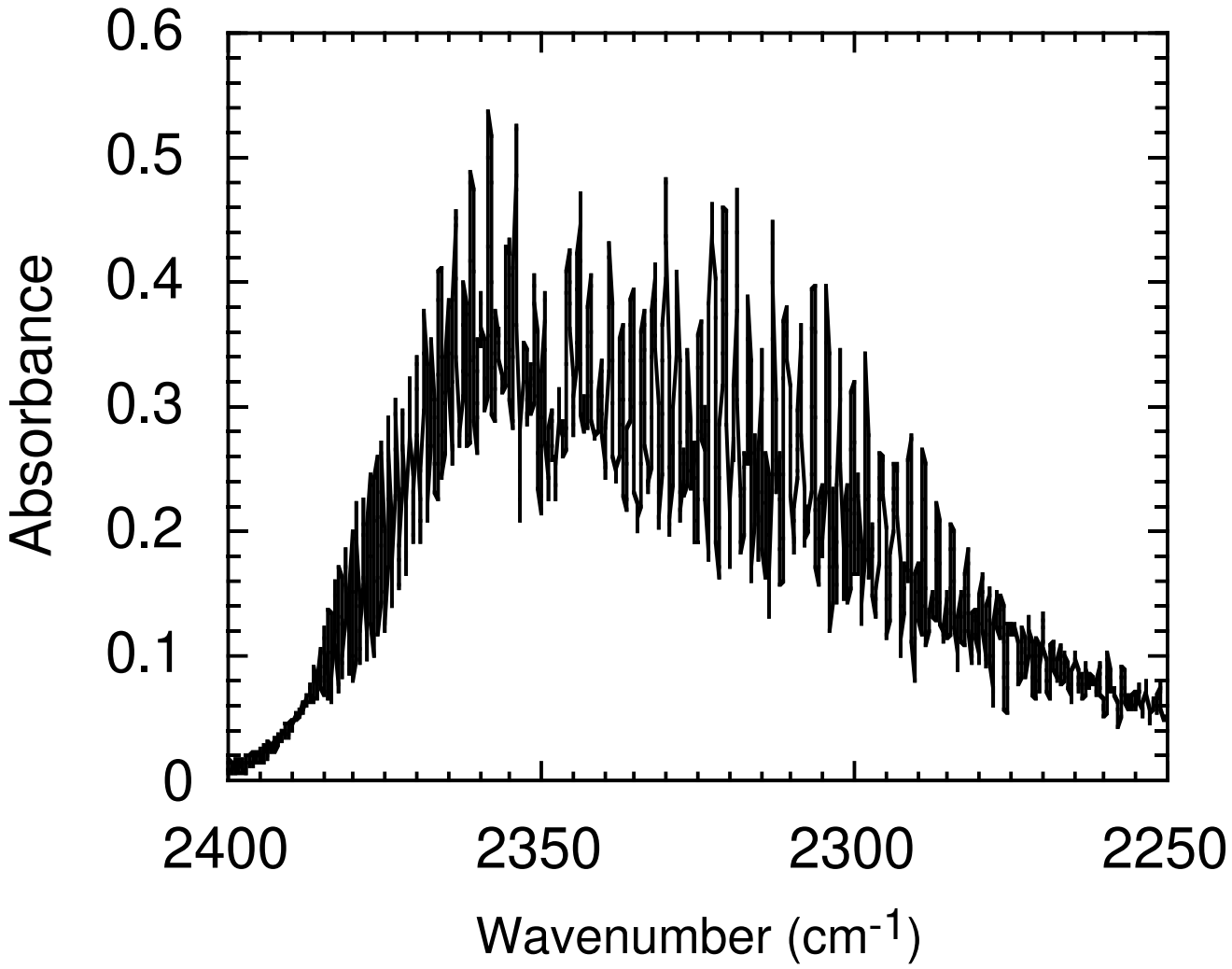

PPPL-3281/Fig. 15: FTIR spectrum of carbon dioxide antisymmetric stretching band at 2349 cm^{-1}.

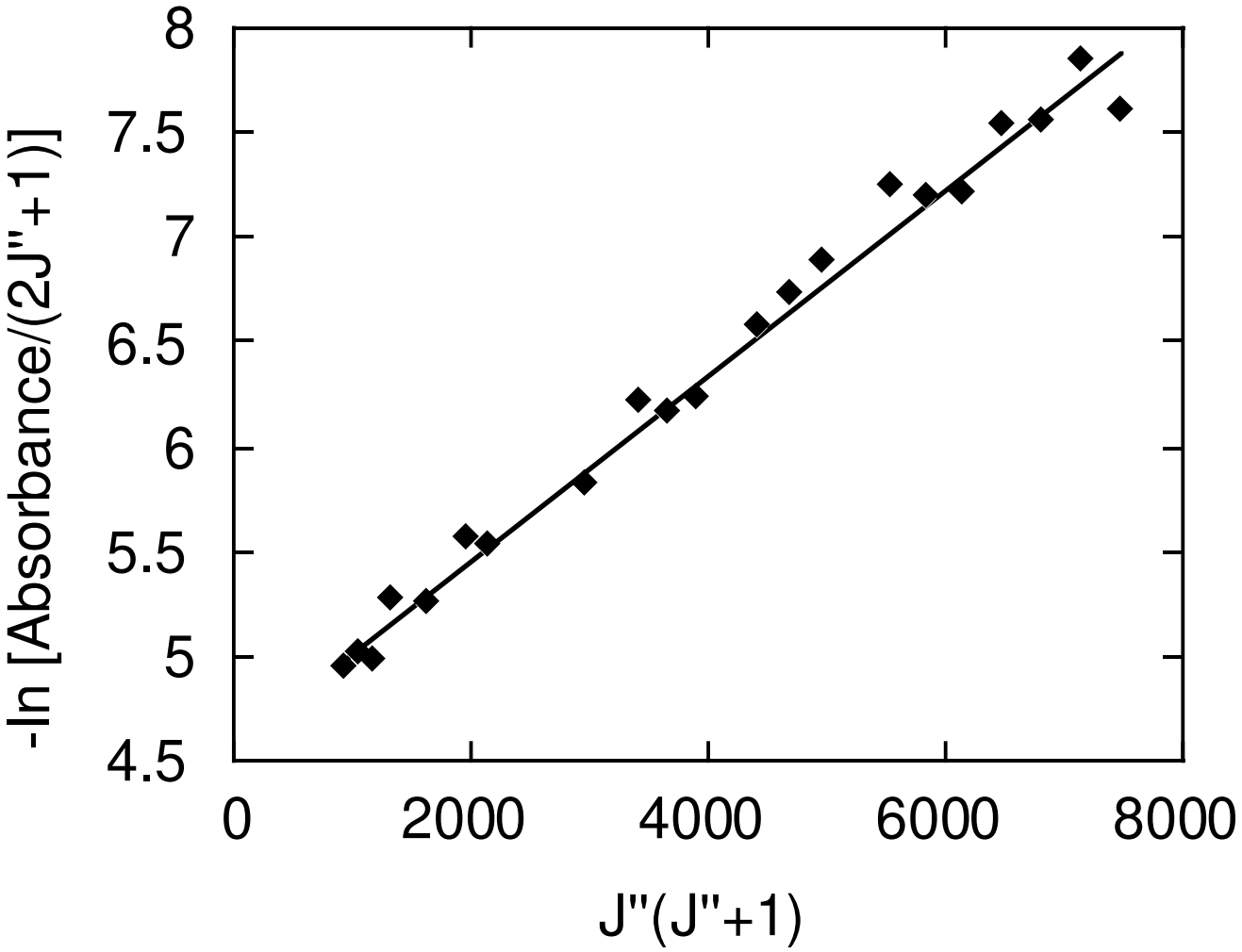

PPPL-3281/Fig. 16: Fit to carbon dioxide P-branch spectrum used to measure rotational temperature.